Shock and Vibration 15 (2008) 383–393
IOS Press

Simple models for the dynamic modeling of rotating tires

J.C. Delamotte, R.F. Nascimento and J.R.F. Arruda*
Departamento de Mecânica Computacional, Universidade Estadual de Campinas, Rua Mendeleiev, s/n, Cidade Universitária "Zeferino Vaz", 13.083-970, Campinas, SP, Brazil

Abstract. Large Finite Element (FE) models of tires are currently used to predict low frequency behavior and to obtain dynamic model coefficients used in multi-body models for riding and comfort. However, to predict higher frequency behavior, which may explain irregular wear, critical rotating speeds and noise radiation, FE models are not practical. Detailed FE models are not adequate for optimization and uncertainty predictions either, as in such applications the dynamic solution must be computed a number of times. Therefore, there is a need for simpler models that can capture the physics of the tire and be used to compute the dynamic response with a low computational cost. In this paper, the spectral (or continuous) element approach is used to derive such a model. A circular beam spectral element that takes into account the string effect is derived, and a method to simulate the response to a rotating force is implemented in the frequency domain. The behavior of a circular ring under different internal pressures is investigated using modal and frequency/wavenumber representations. Experimental results obtained with a real untreaded truck tire are presented and qualitatively compared with the simple model predictions with good agreement. No attempt is made to obtain equivalent parameters for the simple model from the real tire results. On the other hand, the simple model fails to represent the correct variation of the quotient of the natural frequency by the number of circumferential wavelengths with the mode count. Nevertheless, some important features of the real tire dynamic behavior, such as the generation of standing waves and part of the frequency/wavenumber behavior, can be investigated using the proposed simplified model.

Keywords: Spectral elements, curved beam, tire, moving force, critical speed, wavenumber

1. Introduction

Many transportation vehicles use pneumatic tires. Understanding the dynamic behavior of rubber tires is of fundamental importance, as the vibration and noise caused by the interaction of the tire with the vehicle dynamics and with the road surface are critical issues in terms of safety, durability, and the environment [1]. Large Finite Element (FE) models with the detailed geometry of tires are currently used to predict low frequency behavior and to obtain dynamic model coefficients used in multi-body models for riding and comfort [2].

However, in order to predict the high frequency behavior which may explain irregular wear, critical speeds and noise radiation, large FE models are not practical. Even if a very large, refined FE model is built for higher frequency prediction, it will not be adequate for optimization and uncertainty predictions, where the dynamic solution must be computed a large number of times. Therefore, there is a need for simpler, semi-analytical methods that can capture the physics of the tire and, yet, yield simple models that can be used to compute the dynamic response with a very low computational cost. In this paper, the spectral element approach is used to derive such models.

Simple ring models are derived using the spectral element approach [3] and the implementation of a rotating force in such a model is discussed. First, a simple circular beam spectral element is derived and validated by comparing the frequency response to a point force with the analytical solution. Then a circular beam element with string effect is derived. This element allows simulation of the tire internal pressure. The behavior of the ring under different internal pressures is investigated using the modal approach and frequency/wavenumber plots. This behavior is compared with the experimental results obtained with a real, untreaded truck tire. Similarities and differences of the physical behavior of the spectral ring model and the tire are discussed.

*Corresponding author. E-mail: arruda@fem.unicamp.br.

ISSN 1070-9622/08/$17.00

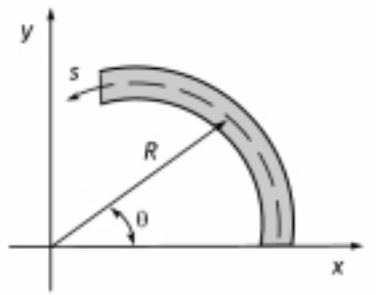

Fig. 1. Scheme of a circular beam.

2. Circular beam spectral element

A curved beam spectral element will be derived in this section. A scheme of a circular beam segment can be seen in Fig. 1.

In this first derivation the internal pressure is not included. This will be done in the next section. The equilibrium equations for the circular beam in cylindrical coordinates may be written as [3,4]:

$$\begin{aligned} EA\frac{\partial^2 u}{\partial^2 s} + \frac{1}{R^2}\left(EI\frac{\partial^2 u}{\partial s^2} - EAR\frac{\partial v}{\partial s} + EIR\frac{\partial^3 v}{\partial s^3}\right) &= \rho A\frac{\partial^2 u}{\partial t^2} \\ EI\frac{\partial^4 v}{\partial s^4} + \frac{1}{R^2}\left(EAv - EAR\frac{\partial u}{\partial s} + EIR\frac{\partial^3 u}{\partial s^3}\right) &= -\rho A\frac{\partial^2 v}{\partial t^2} \end{aligned} \tag{1}$$

where *EA* is the longitudinal rigidity, *EI* is the bending rigidity, ρA in the mass per unit length, R is the beam radius, u and v are the displacements in the radial and longitudinal directions, respectively. Since the coefficients are constant, the spectral relation can be obtained by assuming solutions of the form:

$$u(\theta,t) = C_u e^{i(-\gamma s-\omega t)} \quad v(\theta,t) = C_v e^{i(-\gamma s-\omega t)} \tag{2}$$

where $\gamma = \pm k$ depending on the direction of wave propagation. Substituting Eq. (2) into Eq. (1) gives:

$$\begin{pmatrix} -\left(EA + \frac{EI}{R^2}\right)\gamma^2 + \rho A\omega^2 & \frac{i\gamma}{R}\left(EA + EI\gamma^2\right) \\ \frac{i\gamma}{R}\left(EA + EI\gamma^2\right) & EI\gamma^4 + \frac{EA}{R^2} - \rho A\omega^2 \end{pmatrix} \times \begin{pmatrix} C_u \\ C_v \end{pmatrix} = \begin{pmatrix} 0 \\ 0 \end{pmatrix} \tag{3}$$

The characteristic equation to determine the wavenumbers k is then formed by setting the determinant of this system to zero. The resulting equation is:

$$\frac{1}{\omega}k^6 - (\frac{\rho\omega}{E} + \frac{2}{R^2\omega})k^4 - \left(\frac{\rho A\omega}{EI} + \frac{\rho\omega}{ER^2} - \frac{1}{R^4\omega}\right)k^2 - \left(\frac{1}{R^2 EI} - \frac{\rho\omega^2}{EI\cdot E}\right)\rho A\omega = 0 \tag{4}$$

where the amplitude ratios for each mode are obtained from Eq. (3) as either one of the following equations:

$$\alpha = \frac{C_u}{C_v} = -\frac{\frac{i\gamma}{R}(EA + EI\gamma^2)}{-\left(EA + \frac{EI}{R^2}\right)\gamma^2 + \rho A\omega^2} \text{ or } \alpha = \frac{C_u}{C_v} = -\frac{EI\gamma^4 + \frac{EA}{R^2} - \rho A\omega^2}{\frac{i\gamma}{R}(EA + EI\gamma^2)} \tag{5}$$

For $\gamma = \pm k$, Eq. (5) can be written as:

$$\alpha = \pm\frac{\frac{ik}{R}(EA + EIk^2)}{-\left(EA + \frac{EI}{R^2}\right)k^2 + \rho A\omega^2} \tag{6}$$

The general solution of Eq. (1) can be then obtained in the form:

$$\begin{aligned} v(s,t) &= [C_{v1}e^{-ik_1 s} + C_{v2}e^{-ik_2 s} + C_{v3}e^{-ik_3 s} + C_{v4}e^{ik_1 s} + C_{v5}e^{ik_2 s} + C_{v6}e^{ik_3 s}]\cdot e^{-i\omega t} \\ u(s,t) &= [C_{u1}e^{-ik_1 s} + C_{u2}e^{-ik_2 s} + C_{u3}e^{-ik_3 s} + C_{u4}e^{ik_1 s} + C_{u5}e^{ik_2 s} + C_{u6}e^{ik_3 s}]\cdot e^{-i\omega t} \end{aligned} \tag{7}$$

where,

$$\frac{C_{u1}}{C_{v1}} = \frac{C_u}{C_v}(k_1) = \alpha_1, \frac{C_{u2}}{C_{v2}} = \alpha_2, \frac{C_{u3}}{C_{v3}} = \alpha_3, \frac{C_{u4}}{C_{v4}} = -\alpha_1, \frac{C_{u5}}{C_{v5}} = -\alpha_2, \frac{C_{u6}}{C_{v6}} = -\alpha_3 \tag{8}$$

Substituting Eq. (8) into Eq. (7) gives:

$$\alpha = \begin{pmatrix} \alpha_1 & 0 & 0 & 0 & 0 & 0 \\ 0 & -\alpha_1 & 0 & 0 & 0 & 0 \\ 0 & 0 & \alpha_2 & 0 & 0 & 0 \\ 0 & 0 & 0 & -\alpha_2 & 0 & 0 \\ 0 & 0 & 0 & 0 & \alpha_3 & 0 \\ 0 & 0 & 0 & 0 & 0 & -\alpha_3 \end{pmatrix}, C = \begin{pmatrix} C_1 \\ C_2 \\ C_3 \\ C_4 \\ C_5 \\ C_6 \end{pmatrix}, N(\theta) = \begin{pmatrix} e^{-ik_1 s} \\ e^{-ik_1(s_0-s)} \\ e^{-ik_2 s} \\ e^{-ik_2(s_0-s)} \\ e^{-ik_3 s} \\ e^{-ik_3(s_0-s)} \end{pmatrix} \tag{9}$$

Equation (7) can be represented in the form:

$$v(s) = N^T(s)C; u(s) = N^T(s)\alpha C \tag{10}$$

where u and v are the degrees of freedom of the displacements and $v' = \partial v/\partial s$ is the rotation of the beam section. It is represented in the equation below;

$$\begin{aligned} v' = &-ik_1C_1e^{-ik_1 s} + ik_1C_2e^{-ik_1(s_0-s)} - ik_2C_3e^{-ik_2 s} + ik_2C_4e^{-ik_2(s_0-s)} - ik_3C_5e^{-ik_3 s} \\ &+ik_3C_6e^{-ik_3(s_0-s)} \end{aligned} \tag{11}$$

where, $v'(\theta) = N^{T\prime}(s)C$. For $s = 0$ and $s = s_0$, that is:

$$\begin{pmatrix} v(0) \\ u(0) \\ v'(0) \\ v(s_0) \\ u(s_0) \\ v'(s_0) \end{pmatrix} = \begin{pmatrix} 1 & e^{-ik_1 s_0} & 1 & e^{-ik_2 s_0} & 1 & e^{-ik_3 s_0} \\ \alpha_1 & -\alpha_1 e^{-ik_1 s_0} & \alpha_2 & -\alpha_2 e^{-ik_2 s_0} & \alpha_3 & -\alpha_3 e^{-ik_3 s_0} \\ -ik_1 & ik_1 e^{-ik_1 s_0} & -ik_2 & ik_2 e^{-ik_2 s_0} & -ik_3 & ik_3 e^{-ik_3 s_0} \\ e^{-ik_1 s_0} & 1 & e^{-ik_2 s_0} & 1 & e^{-ik_3 s_0} & 1 \\ \alpha_1 e^{-ik_1 s_0} & -\alpha_1 & \alpha_2 e^{-ik_2 s_0} & -\alpha_2 & \alpha_3 e^{-ik_3 s_0} & -\alpha_3 \\ -ik_1 e^{-ik_1 s_0} & ik_1 & -ik_2 e^{-ik_2 s_0} & ik_2 & -ik_3 e^{-ik_3 s_0} & ik_3 \end{pmatrix} \times \begin{pmatrix} C_1 \\ C_2 \\ C_3 \\ C_4 \\ C_5 \\ C_6 \end{pmatrix} \tag{12}$$

Denoting this system of equations in matrix form, the solution can be written as:

$$U = GC \quad \Rightarrow C = G^{-1}U \tag{13}$$

Equation (13) can now be written as:

$$\begin{pmatrix} v(s) \\ u(s) \\ v'(s) \end{pmatrix} = \begin{pmatrix} N^T(s) \\ N^T(s) \cdot \alpha \\ N^{T\prime}(s) \end{pmatrix} G^{-1}U \tag{14}$$

The spectral components of the axial force, bending moment and transverse shear force are given by [3],

$$N = EA\left(\frac{\partial u}{\partial s} - \frac{v}{R}\right) Q = -EI\left(\frac{1}{R}\frac{\partial^2 u}{\partial s^2} + \frac{\partial^3 v}{\partial s^3}\right) M = EI\left(\frac{1}{R}\frac{\partial u}{\partial s} + \frac{\partial^2 v}{\partial s^2}\right) \tag{15}$$

Substituting Eq. (15) into Eq. (10) and Eq. (11) gives:

$$\begin{aligned} \begin{bmatrix} -N(0) \\ -Q(0) \\ -M(0) \\ N(s_0) \\ Q(s_0) \\ M(s_0) \end{bmatrix} = &\begin{bmatrix} -EA\left(N^{T\prime}(0)\cdot\alpha - \frac{1}{R}N^T(0)\right) \\ EI\left(\frac{1}{R}N^{T\prime\prime}(0)\cdot\alpha + N^{T\prime\prime\prime}(0)\right) \\ -EI\left(\frac{1}{R}N^{T\prime}(0)\cdot\alpha + N^{T\prime\prime}(0)\right) \\ EA\left(N^{T\prime}(s_0)\cdot\alpha - \frac{1}{R}N^T(s_0)\right) \\ -EI\left(\frac{1}{R}N^{T\prime\prime}(s_0)\cdot\alpha + N^{T\prime\prime\prime}(s_0)\right) \\ EI\left(\frac{1}{R}N^{T\prime}(s_0)\cdot\alpha + N^{T\prime\prime}(s_0)\right) \end{bmatrix} G^{-1}U \Rightarrow K = \\ &\begin{bmatrix} -EA\left(N^{T\prime}(0)\cdot\alpha - \frac{1}{R}N^T(0)\right) \\ EI\left(\frac{1}{R}N^{T\prime\prime}(0)\cdot\alpha + N^{T\prime\prime\prime}(0)\right) \\ -EI\left(\frac{1}{R}N^{T\prime}(0)\cdot\alpha + N^{T\prime\prime}(0)\right) \\ EA\left(N^{T\prime}(s_0)\cdot\alpha - \frac{1}{R}N^T(s_0)\right) \\ -EI\left(\frac{1}{R}N^{T\prime\prime}(s_0)\cdot\alpha + N^{T\prime\prime\prime}(s_0)\right) \\ EI\left(\frac{1}{R}N^{T\prime}(s_0)\cdot\alpha + N^{T\prime\prime}(s_0)\right) \end{bmatrix} G^{-1} \end{aligned} \tag{16}$$

where K is the spectral element matrix of the circular beam.

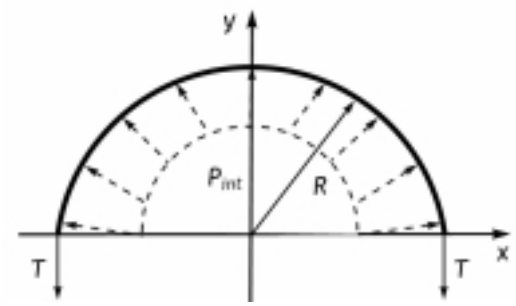

Fig. 2. Free-body diagram of a half ring under internal pressure.

3. Circular beam with internal pressure

In matrix K of Eq. (16) the effect of the internal pressure is not included. It is known that the internal pressure has a strong influence in the tire dynamics. In order to take into account the internal pressure (string effect), tension T will be introduced in Eq. (1).

$$\mu\frac{\partial^2 v}{\partial t^2} = T\frac{\partial^2 v}{\partial s^2} \tag{17}$$

To determine the value of the tension on the beam equivalent to the internal pressure of the tire, the static equilibrium of a section of the tire is illustrated in Fig. 2:

The static equilibrium of the half ring yields $\int_0^{\pi} P_{int}.sin(\theta).b.R.d\theta = 2T$, where R is the radius of curvature and b is width of the tire, so that

$$T = P_{int}.b.R \tag{18}$$

The effect of the internal pressure can be introduced in Eq. (1):

$$\begin{aligned} &EA\frac{\partial^2 u}{\partial^2 s} + \frac{1}{R^2}\left(EI\frac{\partial^2 u}{\partial s^2} - EAR\frac{\partial v}{\partial s} + EIR\frac{\partial^3 v}{\partial s^3}\right) = \rho A\frac{\partial^2 u}{\partial t^2} \\ &EI\frac{\partial^4 v}{\partial s^4} + \frac{1}{R^2}\left(EAv - EAR\frac{\partial u}{\partial s} + EIR\frac{\partial^3 u}{\partial s^3}\right) - \left[T\frac{\partial^2 v}{\partial s^2}\right] = -\rho A\frac{\partial^2 v}{\partial t^2} \end{aligned} \tag{19}$$

Since the coefficients are constant, the spectrum relation can be obtained by assuming solutions of the form:

$$u(\theta,t) = C_u e^{i(-\gamma s-\omega t)}; v(\theta,t) = C_v e^{i(-\gamma s-\omega t)} \tag{20}$$

where $\gamma = \pm k$ indicates the direction of the wave propagation along s. Substituting the Eq. (20) into Eq. (19) gives:

$$\begin{pmatrix} -\left(EA + \frac{EI}{R^2}\right)\gamma^2 + \rho A\omega^2 & \frac{i\gamma}{R}\left(EA + EI\gamma^2\right) \\ \frac{i\gamma}{R}\left(EA + EI\gamma^2\right) & EI\gamma^4 + \frac{EA}{R^2} - \rho A\omega^2 + \left[T\gamma^2\right] \end{pmatrix}\begin{pmatrix} C_u \\ C_v \end{pmatrix} = \begin{pmatrix} 0 \\ 0 \end{pmatrix} \tag{21}$$

The characteristic equation to determine the wavenumber k is then formed by setting the determinant of this system to zero. The resulting equation is:

$$\begin{aligned} &\frac{k^6}{\omega} - \left(\frac{\rho\omega}{E} + \frac{2}{R^2\omega} - \left[T(\frac{1}{EI\omega} + \frac{1}{EAR^2\omega})\right]\right)k^4 - \left(\frac{\rho A\omega}{EI} + \frac{\rho\omega}{ER^2} - \frac{1}{R^4\omega} + \left[\frac{T\rho\omega}{E^2 I}\right]\right)k^2 \\ &\quad - \left(\frac{1}{R^2 EI} - \frac{\rho\omega^2}{EI\cdot E}\right)\rho A\omega = 0 \end{aligned} \tag{22}$$

where the amplitude ratios for each mode are obtained from Eq. (21) as either one of the following equations:

$$\alpha = \frac{C_u}{C_v} = -\frac{\frac{i\gamma}{R}(EA + EI\gamma^2)}{-(EA + \frac{EI}{R^2})\gamma^2 + \rho A\omega^2} \text{ or } \alpha = \frac{C_u}{C_v} = -\frac{EI\gamma^4 + \frac{EA}{R^2} - \rho A\omega^2 + \left[T\gamma^4\right]}{\frac{i\gamma}{R}(EA + EI\gamma^2)} \tag{23}$$

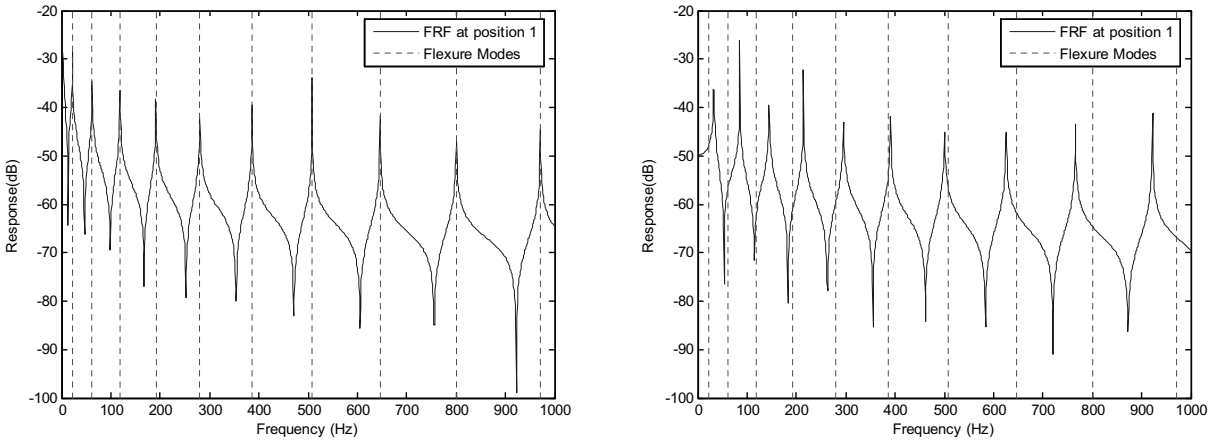

Fig. 3. Circular ring with 2 elements and $P_{int} = 0$ (a), $P_{int} = 3$ bar (b).

The solution of the problem with internal pressure can be obtained analogously to the problem without internal pressure.

Figure 3 shows the forced response of a complete ring with and without internal pressure ($P_{int} = 0$ and $P_{int} = 3$ bar). The dashed vertical lines indicate the analytical natural frequencies of a circular Euler-Bernoulli ring without string effect. These results have been obtained with a model consisting of 2 spectral elements.

4. Wavenumber-frequency analysis

Figure 4 was obtained calculating the wavenumbers at different frequencies. The wavenumber is represented in the x axis and the frequency in the y axis [5]. Magnitudes of the spatial Fourier coefficients are represented by a color bar. The areas of larger values at a certain frequency correspond to the wavenumbers present at that frequency. These usually form lines, and these lines correspond to the spectrum relation $k(\omega)$ of the circular ring. The Fourier coefficients were obtained by applying the spatial Fourier transform to each operational mode. Figure 4(a) was obtained with $P_{int} = 0$ and radial excitation. The curved line corresponds to flexural wave propagation. The straight line corresponds to the compression wave propagation. Figure 4(b) shows the diagram obtained with tangential excitation.

Figures 5(a) and 5(b) show the diagrams obtained with radial excitation with $P_{int} = 3$ bar and $P_{int} = 90$ bar.

The curve of flexural wave propagation does not follow either the theoretical beam curve or the theoretical curve for the circular string. When the internal pressure is larger, the ring behaves more like a string than like a beam.

5. Moving load

The implementation of a rotating force in such a model is discussed in this section. The radial force that moves around the ring with constant angular speed is simulated using a triangular pulse that is applied to each element node subsequently with a delay that corresponds to time that the force takes to move from one node to the next.

The function $f(t)$ which defines the triangular pulse is given by:

$$f(t) = b\left(1 - \frac{t}{a}\right), \quad 0 \leqslant t \leqslant a \text{ and } f(t) = b\left(1 + \frac{t}{a}\right), \quad -a \leqslant t \leqslant 0 \tag{24}$$

The Fourier transform of the triangular pulse is:

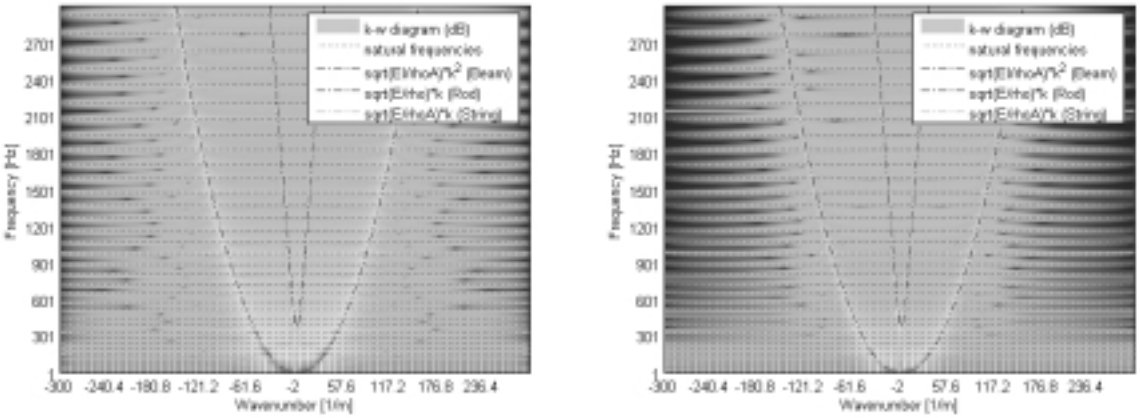

(a) (b)

Fig. 4. Diagrams k-ω with radial excitation (a) and with tangential excitation (b) and $\mathrm{P}_{int} = 0$.

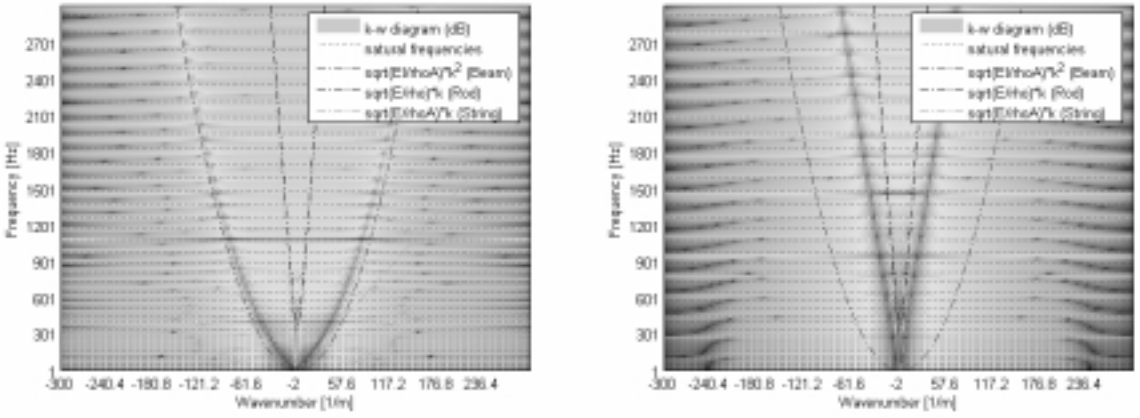

(a) (b)

Fig. 5. Diagrams k-ω with radial excitation and $\mathrm{P}_{int} = 3$ bar (a) and $\mathrm{P}_{int} = 90$bar (b).

$$\mathrm{X}(\omega) = \int_{-a}^{0} b\left(1 + \frac{t}{a}\right) e^{-j\omega t} dt + \int_{0}^{a} b\left(1 - \frac{t}{a}\right) e^{-j\omega t} dt \Rightarrow \mathrm{X}(\omega) = -\frac{b}{a\omega^2}(e^{j\omega a} + e^{-j\omega a} - 2) \tag{25}$$

where $j = \sqrt{-1}$. The pulse applied at each node m must be shifted of a time delay $m\Delta t$ such that:

$$\mathrm{Z}_m(\omega) = \left[-\frac{b}{a\omega^2}(e^{j\omega a} + e^{-j\omega a} - 2)\right] e^{-j\omega m\Delta t} \tag{26}$$

Dividing the Eq. (26) by the period τ we obtain the Fourier coefficients of the triangular pulse. Equation (27) can be interpreted as a way of transforming the periodic signal from the time to the frequency domain to be used in the spectral formulation.

$$a_k = \left[-\frac{b}{a\omega_k^2}(e^{j\omega_k a} + e^{-j\omega_k a} - 2)\right] \frac{e^{-j\omega_k m\Delta t}}{\tau} \tag{27}$$

where $\omega_k = \frac{2\pi k}{\tau}$ and k varies from 1 to the number of Fourier coefficients.

Once the stiffness matrices and the load vector presented in Eq. (27) are obtained in the frequency domain, one can compute the response:

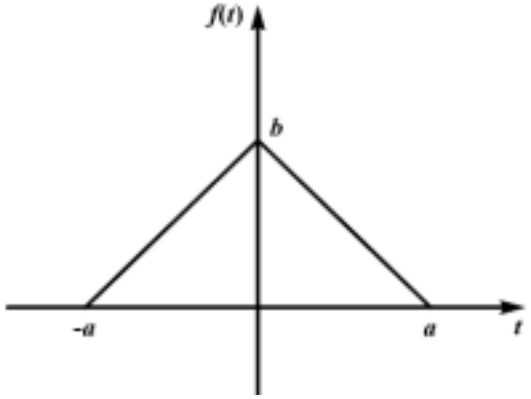

Fig. 6. Triangular pulse.

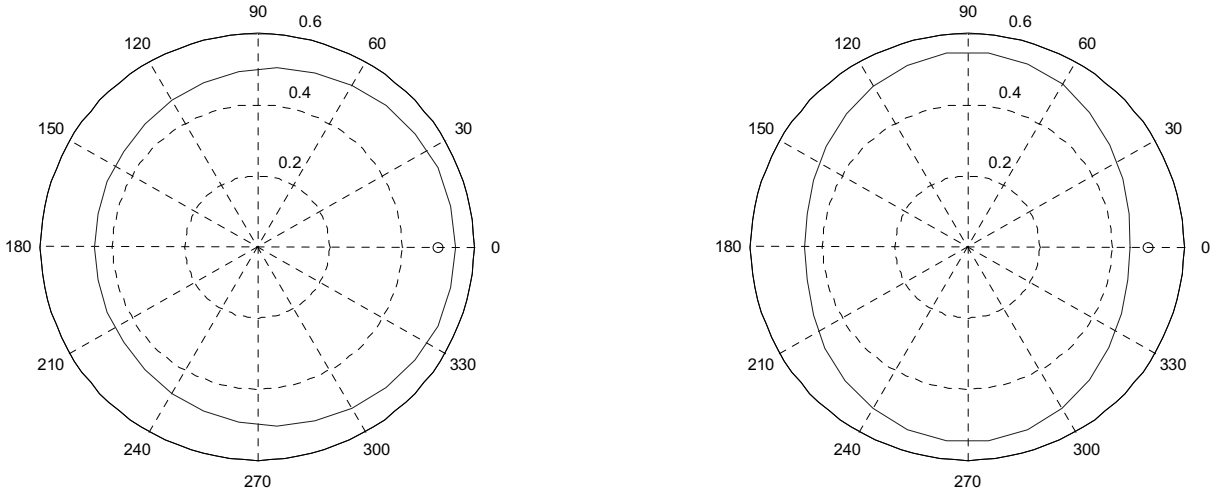

Fig. 7. Mode 1 excited at velocity 31 m/s and mode 2 at velocity 39.2 m/s.

$$X(\omega_k) = K^{-1}(\omega_k)P(\omega_k) \tag{28}$$

where $P(\omega_k)$ is the load vector. To obtain the response in the time domain one can use the expression:

$$x\,(t) = \sum_{k=1}^{M} X\,(\omega_k)\, e^{\frac{j2\pi kt}{\tau}} \tag{29}$$

where M is the number of Fourier coefficients.

Figures 7–9 show some forced responses to rotating forces at different speeds. The speeds have been chosen so that one of the radial modes of the ring is excited. Because of the moving force approximation 30 spectral elements were used to obtain these results.

6. Experimental results

An experimental test was performed with an untreaded truck tire with a non-rotating radial force. The tire mounted on a wheel and the wheel was rigidly fixed. The tread-band was excited in the frequency range from 30 to 800 Hz using an electro-dynamical shaker attached to the tread-band through a stinger and a force transducer. A total of 203

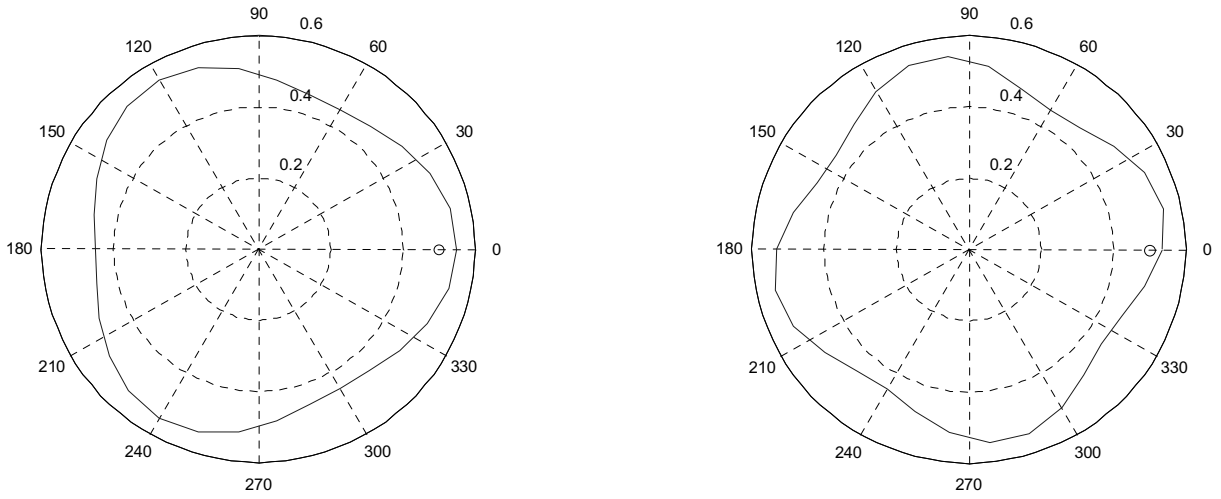

Fig. 8. Mode 3 excited at velocity 41.8 m/s and mode 4 at velocity = 42.9 m/s.

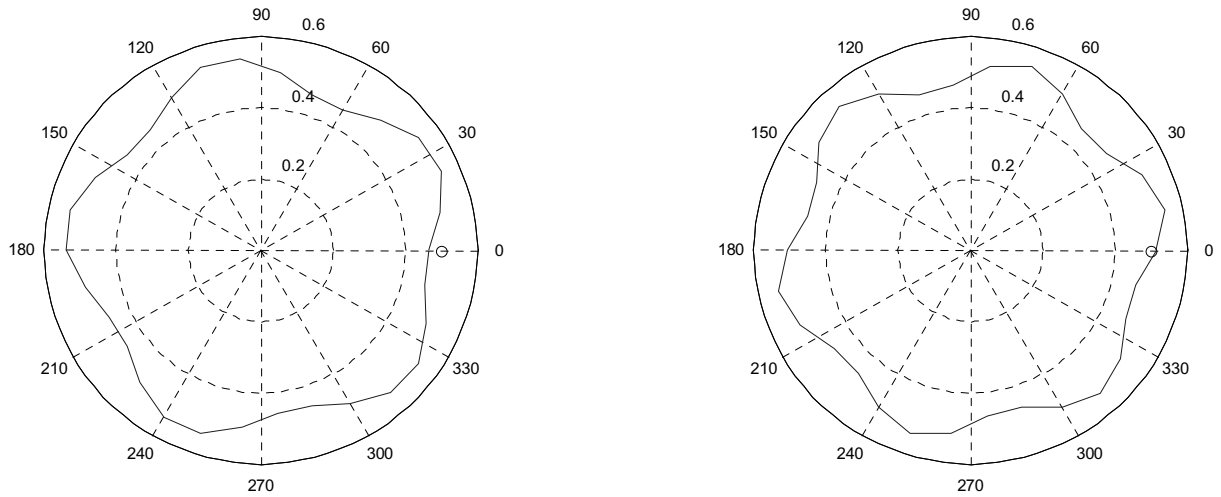

Fig. 9. Mode 5 excited at velocity 43.6 m/s and mode 6 at velocity 44.2 m/s.

points were measured around the tire circumference using a laser Doppler vibrometer. Furthermore, 60 points were measured along a vertical line on the tire tread-band to check for the cross-section propagation mode. The natural frequencies of the tire were obtained from the peaks of the measured Frequency Response Functions. For further details on the experiment see [6]. Using this information a critical speed analysis could be performed. Standing waves appear in the tire when the rotation speed reaches the critical values. These critical values for each mode are reached when the rotation speed coincides with one of the natural frequencies of the tire divided by the number of circumferential wavelengths of the mode n [7],

$$\Omega = \omega_k / n \tag{30}$$

The first critical rotation speed of the tire is reached when the first standing waves are formed, i.e., $\Omega_c = (\omega_k/n)_{\min}$. Figure 10 shows the critical speed diagram for the tire investigated. This simplified analysis does not take into account the influence of the nonlinearities caused by the large deformations of the tire that are present under actual use nor the effect of the centripetal force.

Figure 11 was obtained from the circumferential measurements by calculating the wavenumber spectrum at different frequencies using a spatial Fourier transform. The spatial Fourier transform was applied to each operational

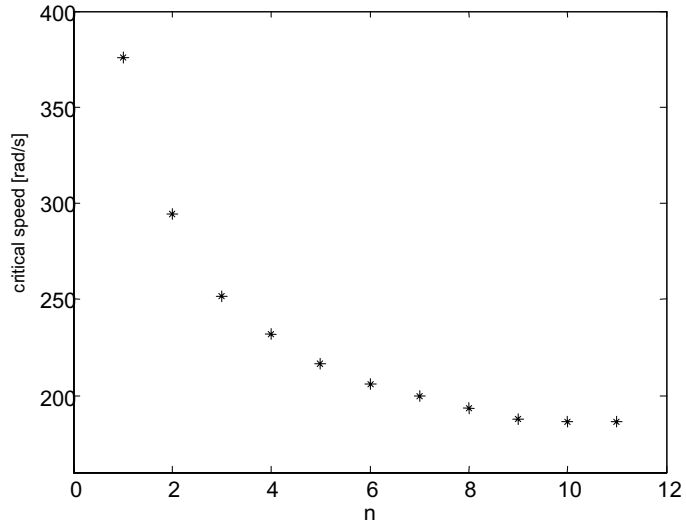

Fig. 10. Critical speed diagram obtained using the first 11 natural frequencies that are associated with cross-section propagation mode $m = 2$.

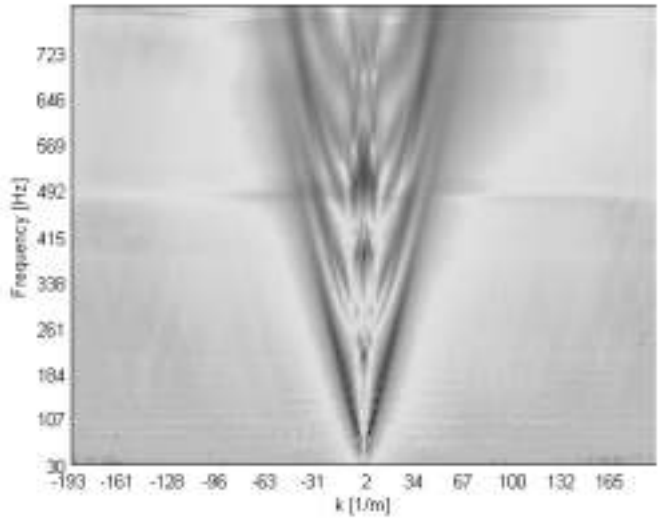

Fig. 11. Diagram k-ω obtained with experimental data for an untreaded truck tire.

mode (as in [5]). The wavenumber is represented on the x axis and the frequency of the operating mode in the y axis. The magnitudes of the Fourier coefficients are represented by a color bar.

7. Critical speed of the circular beam

Figures 11 (a) and (b) present the critical speed diagram for the circular beam with and without internal pressure.

Figure 12 shows the variation of the velocity in relation to the internal pressure (modes 1, 6 and 11). Figure 13 shows an amplitude plot of the radial response of the ring under rotating force excitation as a function of the rotating speed. From this kind of plot, the critical frequency for each mode can be obtained; the plot shown was obtained with an internal pressure $\mathrm{P}_{\mathrm{int}} = 120$ bar.

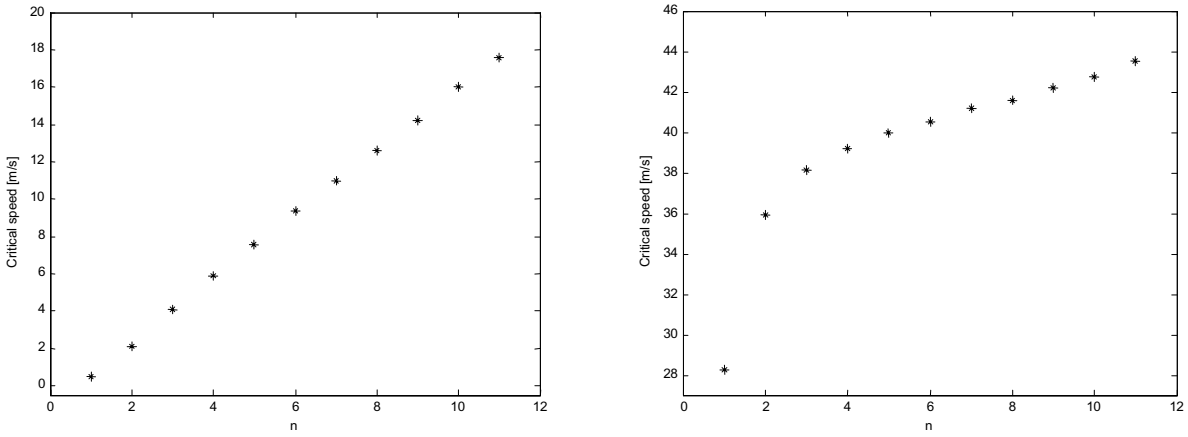

Fig. 12. Critical speed with $P_{int} = 0$ (a) and $P_{int} = 100$ bar.

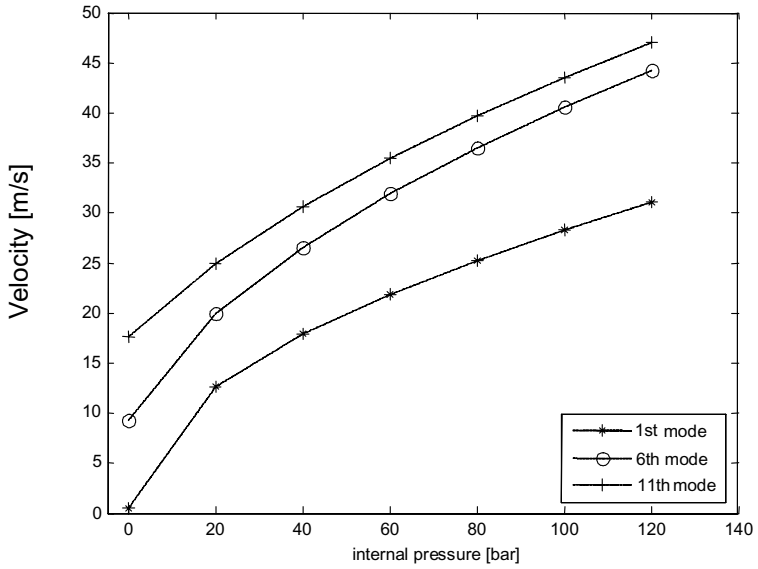

Fig. 13. Influence of pressure on the natural frequencies of modes 1, 6, and 11.

8. Conclusion

In this work, a simplified spectral element model of a circular ring was used to qualitatively model the automotive tire dynamics. A rotating force was implemented and the string effect due to the internal pressure was taken into account. The critical speeds for the excitation of each radial mode were obtained from the rotating force response. Results were compared with experimental results for a real truck tire. Critical speed plots and wavenumber-frequency plots of the simple model and the real tire were obtained. The comparison between simple model predictions and measurements is qualitative. The main purpose of this work is to derive the simplest mechanical model that can explain some of the main dynamical phenomena of an automotive tire regarding standing waves and natural frequencies under a rotating force. As the comparisons were only qualitative, the properties of the beam were not

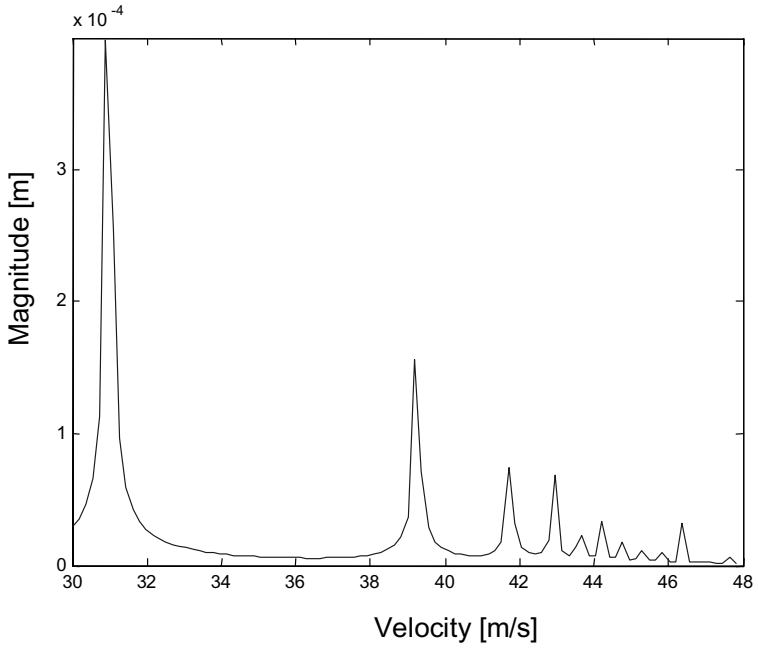

Fig. 14. Magnitude of the response for different rotating force tangential velocities with $P_{\mathrm{int}} = 120$ bar.

derived from the real tire. This can be easily done, however, by statically deforming the real tire or an FE detailed model of it and computing and equivalent bending rigidity.

Acknowledgements

The authors are grateful to the Federal Government research funding agency CNPq for the financial support and to Pirelli tires for proving the untreaded tire used in the experiments.

References

[1] H. Douville, P. Masson and A. Berry, On-resonance transmissibility methodology for quantifying the structure-borne road noise of an automotive suspension assembly, *Applied Acoustics* **67** (2006), 358–382.
[2] J.M.C. Santos, A.L.A. Costa and J.R.F. Arruda, *Truck Tire Finite Element Model Validation by Experimental Modal Analysis*, Proc. of the Int. Conf. on Structural Dynamics Modeling, Funchal, Madeira, Portugal, Jun. 2002, CD-ROM, 11.
[3] J.F. Doyle, *Wave Propagation in Structures*, (2d ed.), A Spectral Analysis Approach, Springer, 1997.
[4] B. Kang, C.H. Riedel and C.A. Tang, Free Vibration Analysis of Planar Curved Beams by Wave Propagation, *Journal of Sound and Vibration* **260** (2003), 19–44.
[5] J.S. Bolton, H.J. Song, Y.K. Kim and D.E. Newland, *The Wave Number Decomposition Approach to the Analysis of Tire Vibration*, Proceedings of NOISE-CON 98, pp. 97–102.
[6] J.C. Delamotte, *Propagation Des Vibrations Dans Le Pneu*, Graduation work report, Ecole Nationale Supérieure d'Ingénieurs du Mans, Le Mans, France, 2006 (in French).
[7] W. Soedel, On The Dynamic Response of Tires According to Thin Shell Approximations, *Journal of Sound and Vibration* **41** (1975), 233–246.